Etched Implants: A Comparative Surface Analysis of Four Implant Systems

S. Szmukler-Moncler,[1,2] T. Testori,[2] J. P. Bernard[1]

[1] Department of Oral Surgery, School of Dental Medicine, University of Geneva, Barthélémy Menn 4, CH-1211 Geneva, Switzerland

[2] Department of Odontology, Section of Implantology and Oral Rehabilitation, Galeazzi Orthopeadic Institut, University of Milano, Milano, Italy

Abstract: Surface texturing by acid etching has recently become popular among dental implant manufacturers. The aim of this study was to compare the surface topography of four implant systems and to check the reproducibility of the industrial process of each implant system. Three implants per system have been selected from three distinct batches. They were observed under a scanning electron microscope (SEM), and roughness was determined with a contact profilometer by measuring five height-descriptive parameters (*Ra*, *Rq*, Rz_{ISO}, *Rt*, and *Rsk*, a texture parameter *Sm*, and a hybrid parameter *RΔq*. The analysis showed that each implant system displayed a distinct surface topography that could not be mistaken. When sandblasting was performed prior to etching, surface topography was a combination of macro- and microroughness. The roughness and the amount of remaining sand varied among the batches, showing that the industrial process is not fully developed. Deviation from the released technical information was found for two out of four implant manufacturers. Based on the available biological and clinical data on textured surfaces, it is suggested that it is bone interlocking at the interface that maintains the biological properties of textured surfaces, rather than a strong implant fixation per se. © 2003 Wiley Periodicals, Inc. J Biomed Mater Res Part B: Appl Biomater 69B: 46–57, 2004

Keywords: acid etching; Osseotite; sandblasting; SLA; surface treatment

INTRODUCTION

Surface state modulates bone response[1–4] and implant anchorage.[5–8] This evidence brought most dental implant manufacturers to switch from the standard machined surface and implement new surface treatments. Recently, acid etching gained in popularity among manufacturers to prepare textured titanium surfaces. Some of these surfaces have been documented to lead to more bone apposition,[1,3,9] to enhance the interfacial strength as measured by removal torque[5,7,8] or push-out tests.[6,10] Furthermore, it is claimed that these etched surfaces can reduce the healing time in the mandible and in the maxilla from 3–6 months to 6–8 weeks.[11–14]

For example, Lazzara et al.[9] compared the bone response to Osseotite and machined surfaces placed in the human posterior maxilla. After 6 months of healing, the bone contact at the Osseotite surface was 72.96%, compared to 33.98% for the machined surface. At the Osseotite surface, a special feature of bone creeping along the etched surface was observed. The osteoconductive effect of the Osseotite textured surface over the machined surface was particularly pronounced in the softer trabecular bone. In this type of bone, the amount of bone apposition was enlarged from 6.5 ± 10.8% for the machined surface to 59.1 ± 25.3% for the Osseotite. Klokkevold et al.[7] compared the anchorage of etched Osseotite and machined surfaces after 1, 2, and 3 months in the rabbit tibia model. After 1 month of healing, the mean removal torque of the machined surface was 6.00 ± 0.64 N cm, whereas for the Osseotite surface it was 21.86 ± 1.37 N cm, that is, 3.6 times higher. After 2 months, the increase was 3.0 times, and after 3 months, the etched surface required a removal torque of 27.40 ± 3.89 N cm versus 6.73 ± 0.95 N cm for the machined surface (× 4.1).

Acid etching is a subtractive method, wherein pits are created in the titanium surface. The surface topography obtained by acid attack can be modulated according to prior treatment, for example, sandblasting, using acid mixtures, using different temperatures, and using different etching times. The aim of this survey was twofold: (a) to compare the etched surface topography of four distinct implant systems,

Correspondence to: Serge Szmukler-Moncler, Blauensteinerstrasse 8, CH-4053 Basel, Switzerland (e-mail : ssm@bluewin.ch)

TABLE I. Characteristics of the Investigated Implants and Implant Systems

	Osseotite	SLA	DPS	HaTi
Implant length	8.5 mm	8 mm	11 mm	11 mm
Lot number	39504	1005	940301510069	5002
Expiration of sterilization date	November 2002	July 2003	December 1998	April 2004
Implant length	10 mm	10 mm	13 mm	14 mm
Lot number	41559	1010	940333310072	5001
Expiration of sterilization date	December 2002	September 2003	December 1998	July 2005
Implant length	13 mm	12 mm	15 mm	17 mm
Lot number	71022	1009	970040210208	N5004
Expiration of sterilization date	August 2003	October 2003	June 2001	July 2004

(b) to check for the reproducibility of the industrial process of each implant system.

MATERIAL AND METHODS

Implants

Commercially available implants from four implant systems were investigated. Three implants per system were randomly chosen. Three different lengths of implants were examined, each one with a different lot number and a distinct sterilization date (Table I). This was to ensure that the implants were manufactured from three distinct batches.

DPS-Frialit II implant. This implant system is manufactured by Friatech AG (Mannheim, D). The system is reported to have been sandblasted and acid etched since 1989.[15] No details about the etching process have been found in the literature or in the manufacturer's advertisements. Because this surface has been available since 1989, implants created over a large time span were collected. Implants were 3.8 mm in diameter and 11, 13, and 15 mm in length. Corresponding lot numbers were 940301510069, 940333310072, and 970040210208; sterilization expiration dates were 12.1998, 12.1998, and 06.2001, respectively, as shown in Table I.

Osseotite implant. This implant system is manufactured by 3i (Palm Beach Gardens, FL). According to Beaty,[16] a dual thermo-etching is performed; that is, the implant surface is successively immersed in a 15% HF bath to remove the native titanium oxide layer and then etched in a mixture of H_2SO_4/HCl acids (ratio of 6:1), and heated at 60–80 °C for 3–10 min to create the surface texture. The implants were 4.0 mm in diameter and 8.5, 10, and 13 mm in length. Lot numbers were, respectively, 39504, 41559 and 71022. Sterilization expiration dates were 11.2002, 12.2002, and 08.2003, respectively, as shown in Table I.

SLA-ITI implant. This implant system is manufactured by Straumann AG (Waldenburg, CH). According to Steinemann and Claes,[17] the implant surface is sandblasted with large grit (0.25–0.50 mm) alumina and etched in a boiling mixture of HCl/H2SO4. Etching conditions of 125–130 °C and 5 min have been reported by Wong et al.[6] The implants were 4.1 mm in diameter and 8, 10, and 12 mm in length. Lot numbers were 1005, 1010, and 1009, respectively. Corresponding sterilization expiration dates were 07.2003, 09.2003, and 10.2003, respectively, as shown in Table I.

HaTi implant. This implant system is manufactured by HaTi Dental AG (Bettlach, CH). According to the manufacturer, the implant is sandblasted and etched. No record of the etching process was found in the literature or in the manufacturer's advertisements. Implants were 4.2 mm in diameter and 11, 14, and 17 mm in length, respectively. Lot numbers were 5002, 5001, and N5004. Corresponding sterilization expiration dates were 04.2005, 07.2005, and 07.2004, respectively, as shown in Table I.

Roughness Measurement

Implant roughness measurement was performed with a Hommel T8000 profilometer (Hommel AG, Hamburg, D). The measured length was 1.00 mm, cut-off was 0.08 mm, the radius tip was 5 μm, and the filter used was M1 of DIN 4777. The measurements were performed in the same region, preferably at the implant apex, where a flat surface was found, compatible with the measured length.

Six measurements were performed at each implant; they included three statistical height-descriptive parameters, *Ra*, *Rq*, *Rsk*, two extreme height-descriptive parameters, Rz_{ISO}, *Rt*, one texture-descriptive parameter *Sm*, and one hybrid-descriptive parameter, $R\Delta q$. *Ra* is the arithmetic average of the absolute deviation from the mean line over a sampling length, given in micrometers. *Rq* is the root mean square value of the profile departure, given in micrometers. This parameter is more sensitive to extreme values than the *Ra*. *Rq*

TABLE II. Roughness Data of All Implants

	Osseotite	HaTi	DPS	SLA
Implant length	8.5 mm	11 mm	11 mm	8 mm
Ra [μm]	0.46 ± 0.06	0.88 ± 0.08	1.50 ± 0.20	1.56 ± 0.27
Rq [μm]	0.86 ± 0.06	1.63 ± 0.22	3.80 ± 0.34	3.49 ± 0.58
Rz_{ISO} [μm]	3.31 ± 0.53	4.83 ± 0.43	8.27 ± 1.03	8.19 ± 1.19
Rt [μm]	4.97 ± 0.57	6.33 ± 0.63	12.12 ± 2.37	10.04 ± 1.77
Rsk	−1.19 ± 0.42	−0.14 ± 0.24	0.042 ± 0.15	0.052 ± 0.34
Sm [μm]	34.0 ± 4.6	37.5 ± 5.3	64.0 ± 4.4	50.9 ± 9.1
RΔq [rad]	0.191 ± 0.03	0.288 ± 0.03	0.436 ± 0.08	0.50 ± 0.06
Implant length	10 mm	14 mm	13 mm	10 mm
Ra [μm]	0.42 ± 0.08	0.98 ± 0.12	1.56 ± 0.08	1.57 ± 0.18
Rq [μm]	0.733 ± 0.18	1.73 ± 0.17	3.61 ± 0.30	4.26 ± 0.37
Rz_{ISO} [μm]	3.08 ± 0.96	5.41 ± 0.48	8.49 ± 0.51	8.38 ± 0.84
Rt [μm]	4.58 ± 1.45	7.03 ± 0.63	12.27 ± 1.21	11.42 ± 0.94
Rsk	−1.35 ± 0.81	−0.245 ± 0.24	−0.141 ± 0.26	−0.150 ± 0.38
Sm [μm]	27.0 ± 3.2	38.2 ± 8.6	62 ± 5.8	68.8 ± 9.5
RΔq [rad]	0.184 ± 0.04	0.29 ± 0.02	4.33 ± 0.04	0.451 ± 0.06
Implant length	13 mm	17 mm	15 mm	12 mm
Ra [μm]	0.41 ± 0.03	0.85 ± 0.10	1.17 ± 0.10	1.30 ± 0.11
Rq [μm]	0.725 ± 0.10	1.59 ± 0.13	2.69 ± 0.47	3.180 ± 0.036
Rz_{ISO} [μm]	2.51 ± 0.26	4.88 ± 0.47	6.70 ± 0.67	7.15 ± 0.78
Rt [μm]	3.58 ± 0.84	6.22 ± 0.84	10.54 ± 1.73	10.11 ± 0.92
Rsk	−0.016 ± 0.21	−0.306 ± 0.24	−0.16 ± 0.25	0.036 ± 0.29
Sm [μm]	32.0 ± 7.3	38.2 ± 3.7	59.0 ± 1.0	55.8 ± 17.00
RΔq [rad]	0.147 ± 0.01	0.26 ± 0.02	0.357 ± 0.05	0.42 ± 0.04
All implants	All	All	All	All
Ra [μm]	0.43 ± 0.07	0.90 ± 0.11	1.41 ± 0.22	1.48 ± 0.23
Rq [μm]	0.772 ± 0.13	1.65 ± 0.18	3.37 ± 0.61	3.65 ± 0.63
Rz_{ISO} [μm]	2.97 ± 0.70	5.04 ± 0.51	7.82 ± 1.10	7.91 ± 1.05
Rt [μm]	4.38 ± 1.13	6.52 ± 0.76	11.64 ± 1.92	10.52 ± 1.37
Rsk	−0.851 ± 0.79	−0.23 ± 0.24	−0.087 ± 0.23	−0.021 ± 0.33
Sm [μm]	31.0 ± 5.8	38.0 ± 5.8	61.4 ± 5.6	58.5 ± 14.0
RΔq [rad]	0.174 ± 0.03	0.28 ± 0.03	0.41 ± 0.07	0.45 ± 0.06

has a statistical significance as the standard deviation of the height distribution. *Rsk* is the skewness, a number without units; it measures the symmetry of the deviation from a mean plane. A negatively skewed surface has more valleys than peaks; a positively skewed surface has more peaks than valleys. For an equal number of peaks and valleys, the skewness is 0. Skewness is useful to distinguish between asymmetrical profiles of same *Ra* or *Rq*.

Rz_{ISO} is the arithmetic average of the five highest profile peaks and the five lowest profile valleys over the entire measurement trace, given in micrometers. This parameter is sensitive to the changes of pronounced topographic features. *Rt* is the maximum peak to valley of the entire measurement trace, given in micrometers. Large variation of this extreme parameter may be indicative of poor processing or scratches on the surface. *Sm* is the arithmetic average spacing between the falling flanks of peaks on the mean line measured over the sampling length, given in micrometers. *R*Δq is the root-mean-square slope of the profile over the measured length, given in radians.

Scanning Electron Microscopy

The implants were observed with a Philips XL 20 scanning electron microscope. Implants were fixed to an aluminum sample holder on a conducting paste with the long axis parallel to the implant holder. Implants were removed from their sterile package and fixed to the implant holder just before placement in the microscope chamber. Observation was conducted at 20 keV with a taking-off angle of 30 degrees; magnification varied from × 17 to × 4000.

Statistical Analysis

All roughness parameters were compared within a given implant system and pairwise compared between implant systems. After checking normality, the nonparametrical Kruskal-

TABLE III. Statistical Analysis of the Roughness Parameters among the 3 Implants of a Given System. Only the HaTi Implant Had All 3 Implants Similar in Roughness for All 7 Measurements. The Other Implants had 2 to 4 Parameters that Showed Statistically Significant Differences between Implants. S = Statistically Significant Difference between the 3 Implants, NS = No Statistically Significant Difference Between the 3 Implants.

	Osseotite	SLA	DPS	HaTi
Ra [μm]	$p = 0.29$ NS	$p = 0.04$ S	$p = 0.006$ S	$p = 0.13$ NS
Rq [μm]	$p = 0.06$ NS	$p = 0.01$ S	$p = 0.005$ S	$p = 0.40$ NS
Rz_{ISO} [μm]	$p = 0.03$ S	$p = 0.08$ NS	$p = 0.009$ S	$p = 0.10$ NS
Rt [μm]	$p = 0.04$ S	$p = 0.11$ NS	$p = 0.14$ NS	$p = 0.13$ NS
Rsk	$p = 0.005$ S	$p = 0.60$ NS	$p = 0.24$ NS	$p = 0.40$ NS
Sm [μm]	$p = 0.06$ NS	$p = 0.08$ NS	$p = 0.27$ NS	$p = 0.70$ NS
$R\Delta q$ [rad]	$p = 0.02$ S	$p = 0.05$ NS	$p = 0.04$ S	$p = 0.10$ NS

Wallis test (ANOVA) that compares three groups of data or more was used to evaluate any significant roughness difference within an implant system. The Wilcoxon rank-sum test that compares two independent groups was used to pairwise compare the roughness parameters between implant systems. Statistical significance was set at $\alpha = 5\%$.

RESULTS

Roughness Measurement

The mean *Ra*, *Rq*, Rz_{ISO}, *Rt*, *Rsk*, *Sm*, and $R\Delta q$ of the three implants of each implant system ($n = 6$) are given in Table II as well as the corresponding mean values for each implant system ($n = 18$). Statistically significant differences between implants of a given system are shown in Table III.

DPS-Frialit II implant. A statistically significant difference between the three implants was found for the *Ra*, *Rq*, Rz_{ISO} and $R\Delta q$ parameters. No significant difference was found for the *Rt*, *Rsk* and *Sm* (Table III).

Osseotite implant. A statistically significant difference between the three implants was found for the Rz_{ISO}, *Rt*, *Rsk*, and $R\Delta q$ parameters. No significant difference was found for the *Ra*, *Rq*, and *Sm* (Table III).

SLA-ITI implant. A statistically significant difference between the three implants was found for the *Ra* and *Rq* parameters. No significant difference was found for the Rz_{ISO}, *Rt*, *Rsk*, *Sm* and $R\Delta q$ (Table III).

HaTi implant. No significant difference was found for any roughness parameter (Table III).

Comparing the roughness between implant systems. For most parameters (*Ra*, *Rq*, Rz_{ISO}, *Rt*, *Sm*), the roughness order, from smoothest to roughest, was the following: Osseotite < HaTi < DPS < SLA; however, the DPS and SLA implant systems were not statistically significant except for the $R\Delta q$ (Table IV). For the *Rsk*, the Osseotite showed the strongest negative value, decreasing then for the HaTi, the DPS, and the SLA implants; however, only the Osseotite was statistically different from the others (Table IV).

Scanning Electron Microscopy

DPS-Frialit II implant. All implants displayed the same surface feature [Figures 1(a)–1(c)]. Unexpectedly, two distinct surfaces patterns were observed [Figure 1(d)]. The tips of the threads and the flat cervical and apical areas were sandblasted [Figures 1(e) and 1(f)], whereas the thread core

TABLE IV. Pairwise Comparison of the Roughness Parameters Among Implant Systems. S = Statistically Significant, NS = Not Statistically Significant. N and NS Indicate if the Difference Found Between Implant Systems is Significant or Not.

Ra [μm]	Osseotite	S	HaTi	S	DPS	NS	SLA
	0.43 ± 0.07	<	0.90 ± 0.11	<	1.41 ± 0.22	<	1.48 ± 0.23
Rq [μm]	Osseotite	S	HaTi	S	DPS	NS	SLA
	0.772 ± 0.13	<	1.65 ± 0.18	<	3.37 ± 0.61	<	3.65 ± 0.63
Rz_{ISO} [μm]	Osseotite	S	HaTi	S	DPS	NS	SLA
	2.97 ± 0.70	<	5.04 ± 0.51	<	7.82 ± 1.10	<	7.91 ± 1.05
Rt [μm]	Osseotite	S	HaTi	S	SLA	NS	DPS
	4.38 ± 1.13	<	6.52 ± 0.76	<	10.52 ± 1.37	<	11.64 ± 1.92
Rsk	Osseotite	S	HaTi	NS	DPS	NS	SLA
	−0.851 ± 0.79	<	−0.23 ± 0.24	<	−0.087 ± 0.23	<	−0.021 ± 0.33
Sm [μm]	Osseotite	S	HaTi	S	SLA	NS	DPS
	31.0 ± 5.8	<	38.0 ± 5.8	<	58.5 ± 14.0	<	61.4 ± 5.6
$R\Delta q$ [rad]	Osseotite	S	HaTi	S	DPS	S	SLA
	0.174 ± 0.03	<	0.28 ± 0.03	<	0.41 ± 0.07	<	0.45 ± 0.06

area (between the threads) was not roughened by the sandblasting process [Figures 1(d) and 1(g)]. Etching was very weak and did not create noticeable deep pits at either the sandblasted [Figures 1(f) and 1(h)] or the non-sandblasted areas [Figure 1(g)]. A considerable number of small alumina particles were found in the sandblasted areas [Figures 1(e) and 1(g)]. Nevertheless, the implant surface appeared reproducible. In general, the textured surface had only a limited

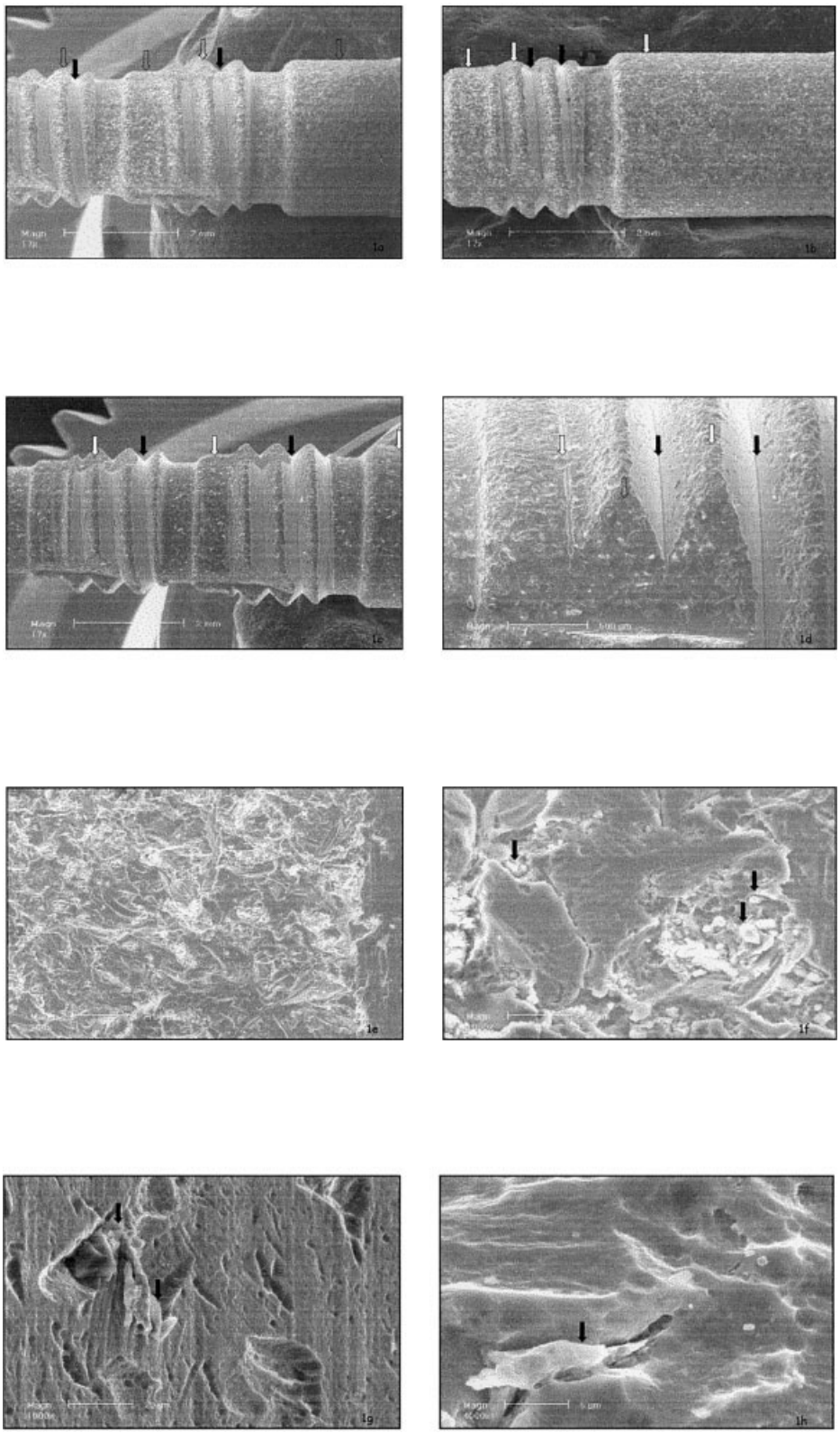

Figure 1.

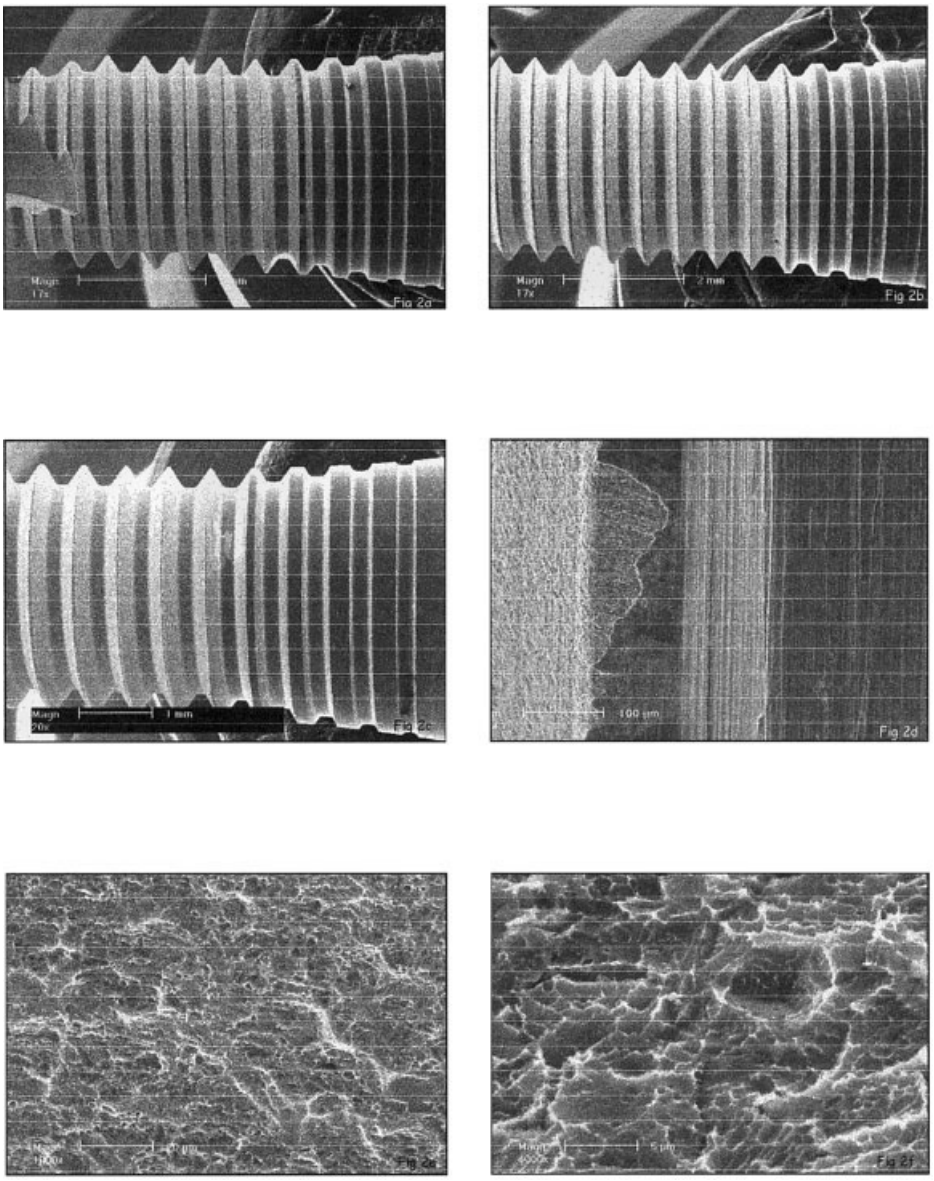

Figure 2. SEM micrographs of the Osseotite implant surface. General overview of (a) the 8.5–mm-long implant, (b) the 10-mm-long implant, and (c) the 13-mm-long implant. Note the machined and the etched areas (× 17).(d) View of the transition zone between the machined and the etched surfaces (× 200). (e) Moderate etching with consistent pits as viewed at high magnification (× 1000). (f) Pits obtained by the dual-thermo etching process as viewed at high magnification (× 4000).

Figure 1. SEM micrographs of the DPS-Frialit II implant surface. General overview of (a) the 11-mm-long implant, (b) the 13-mm-long implant, and (c) the 15-mm-long implant. The white spots correspond to alumina particles (× 17). The white arrows correspond to the blasted areas; the black arrows correspond to the non-blasted area between the threads. (d) Blasted and non-blasted areas. The non-blasted zone corresponds to the interthread area (× 50). The white arrows correspond to the blasted areas; the black arrows correspond to the non-blasted area between the threads. (e) Sandblasted aspect of the surface. The white spots are particles of alumina (× 200). (f) Sandblasted and etched area at high magnification (× 1000). Etching is weak with limited pits. Alumina particles (black arrows) are left weakly attached on the surface. (g) Non-sandblasted area at high magnification (× 1000). The pits are small and do not permit bone ingrowth. Even in this region, some alumina particles have been found (black arrows). (h) Textured surface at high magnification (× 4000). Etching is very weak.

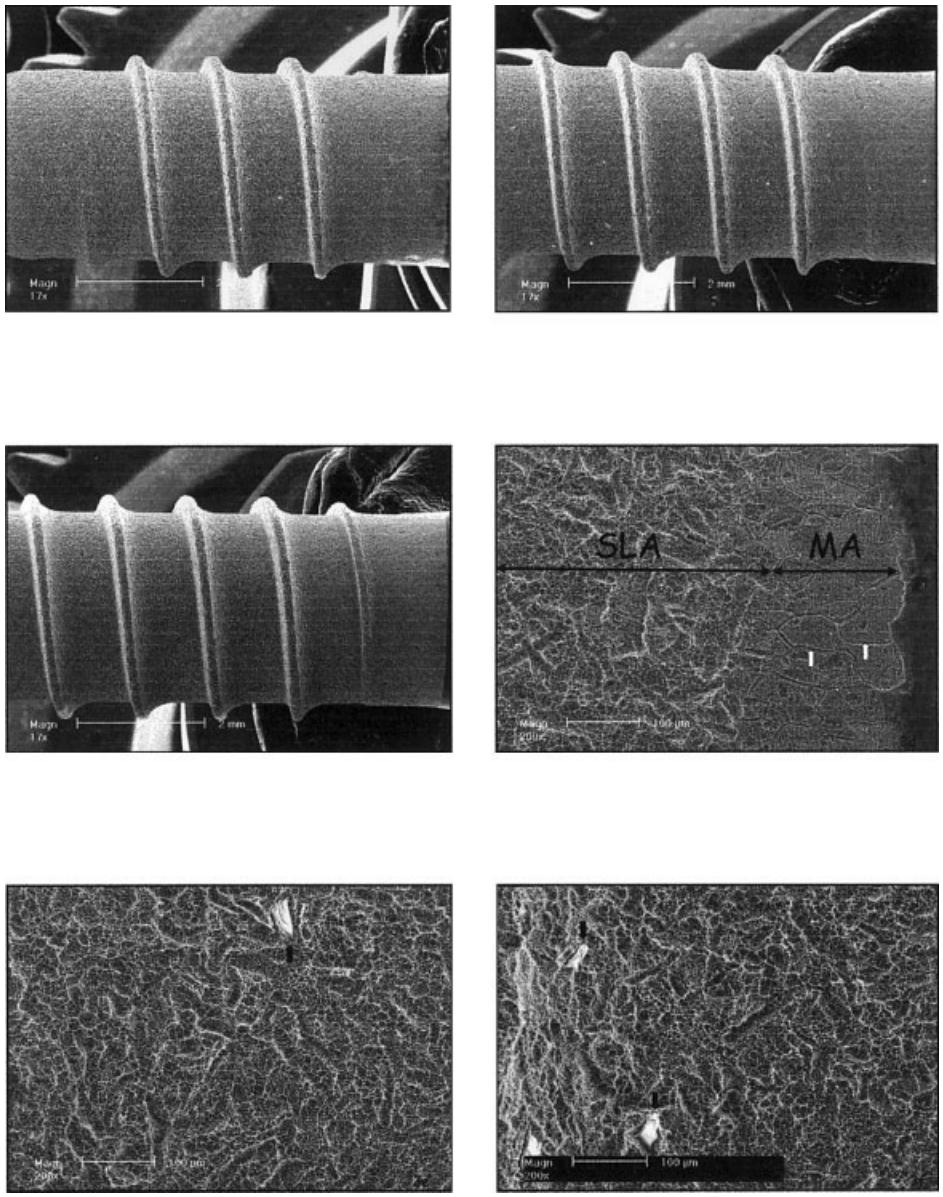

Figure 3. SEM micrographs of the SLA-ITI implant surface. General overview of (a) the 8–mm-long implant, (b) the 10-mm-long implant, and (c) the 12-mm-long implant The white spot corresponds to alumina particles (× 17). (d) Transition zone between the neck and the SLA surface. This area was not sandblasted. Note that the grain boundaries (white arrows) of the metal are revealed (× 200). (e) Macroroughness of the 8-mm-long implant. The white part (black arrow) corresponds to a particle of alumina (× 200). (f) Macroroughness of the 10–mm-long implant. It seems less rough than the 8–mm-long implant surface. The white spots (black arrow) correspond to a particle of alumina (× 200). (g) Macroroughness of the 12–mm-long implant. This implant seems to be the smoothest of the three implants (× 200). Note the grain boundaries (white arrows). (h) Macroroughness and microroughness at high magnification (× 1000). Note the deep pits obtained by etching. The white spots correspond to an alumina particle. (i) Microroughness of the SLA surface. Note the deep pits and undercuts that allow for bone ingrowth (× 4000). (j) Microroughness of the non-sandblasted area (MA). Note the deep pits (× 4000).

micro-scale roughness, without any significant number of sharp, deep pits.

Osseotite implant. As expected, two distinct surfaces patterns were observed. The three cervical threads were left machined, and the apical rest was etched [Figures 2(a)–2(d)]. Etching was moderate and produced pits at the implant surface [Figures 2(e) and –2(f)]. No foreign particles were found; implant surface looked reproducible. A micro-roughness with sharp pits composed the textured surface.

SLA-ITI implant. A distinct amount of remaining blasted particles was found at each implant [Figures 3(a)–3(c)]. Unexpectedly, two distinct surfaces patterns were

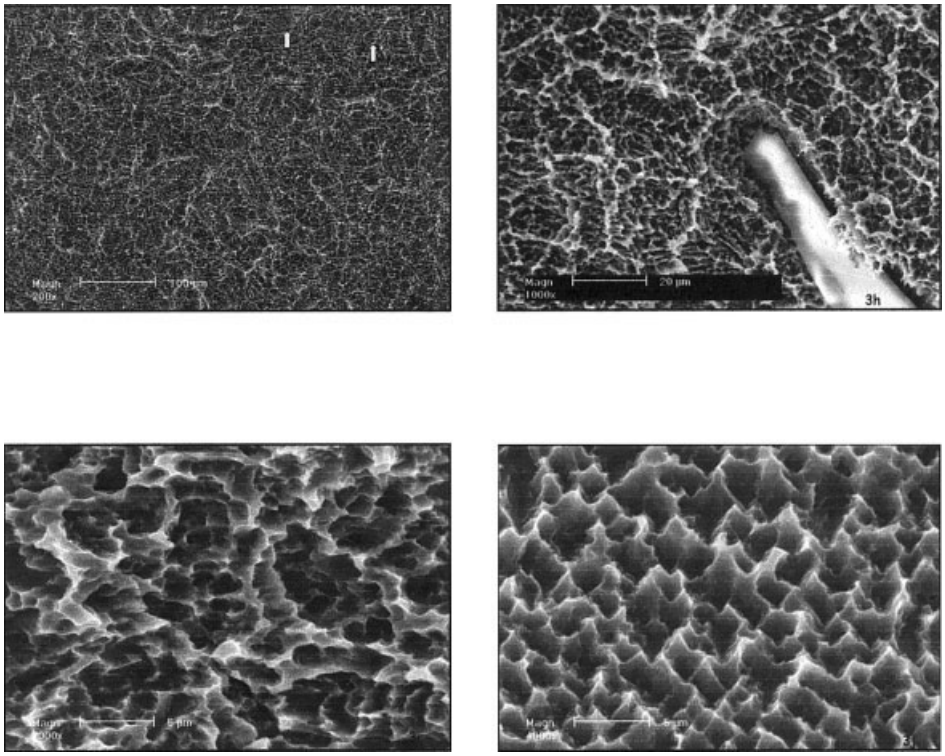

Figure 3. (continued)

observed. A transition zone of approximately 200 μm was consistently found at all implants between the implant neck and the sandblasted-and-etched area [Figure 3(d)]. This region was not sandblasted; it was machined and etched (MA), revealing the grain boundary of the metal [Figure 3(d)]. Each implant displayed a distinct macroroughness [Figures 3(e)–3(g)], whereas the microroughness seemed to be similar [Figures 3(h) and 3(i)]. A rougher surface aspect seemed to correlate with a higher amount of remnant particles. Etching was strong and produced substantial pits both at the SLA [Figure 3(i)] and at the MA areas [Figure 3(j)]. Implant surface was not reproducible. A macro- and microroughness with sharp pits composed the textured surface.

HaTi implant. Each implant displayed a distinct amount of remaining sandblasted particles [Figures 4(a)–4(c)]. Only one surface pattern was observed. Acid attack was strong and produced a macroroughness with pits [Figures 4(d) and 4(e)]. At higher magnification, the pits appeared to be wide and rounded, without undercuts [Figures 4(e) and –4(f)]. The implant surface looked reproducible. A macro- and microroughness with rounded pits composed the textured surface.

DISCUSSION

Probe sampling of three implants, each one from a distinct batch, is insufficient to demonstrate the reproducibility of an industrial process. However, if such a limited probe sampling leads to dissimilar results, it is sufficient to prove the lack of reproducibility of the industrial process. This was the case for three out of the four implant systems. The sandblasted samples showed the largest variability in surface appearance. This might be due to an inappropriate refreshing cycle of the used sand particles. Indeed, during the blasting process, a fraction of the impinging alumina particles are broken into smaller pieces. This blasting material can be either discarded after a single run or further used to roughen more implants. In the latter case, certain implants are blasted with fresh and larger particles, and other implants are blasted with used and smaller particles. Used blasting material is unable to create the same roughness as with fresh blasting material, with its larger particles.

Three implant systems presented a combination of macro- and microroughness, and one presented a combination of machined surface and microroughness. Although the ultimate aim of acid attack is to create pits to allow for bone ingrowth, etching varied from weak to strong. The DPS-Frialit II implant acid treatment produced pits too small to permit bone ingrowth, as shown in Figures 1(f) and 1(h). This surface aspect is caused by the use of either a weak acid mixture, a low etching temperature, or a short etching time. In the blasted areas of this implant, the topography resembled a sandblasted surface rather than etched. The lack of sandblasting between the threads was unexpected; an inadequate orientation of the sandblasting nozzles probably prevented the sand particles from reaching the interthread area. Mention of this surface feature was not found either in the literature[15] or

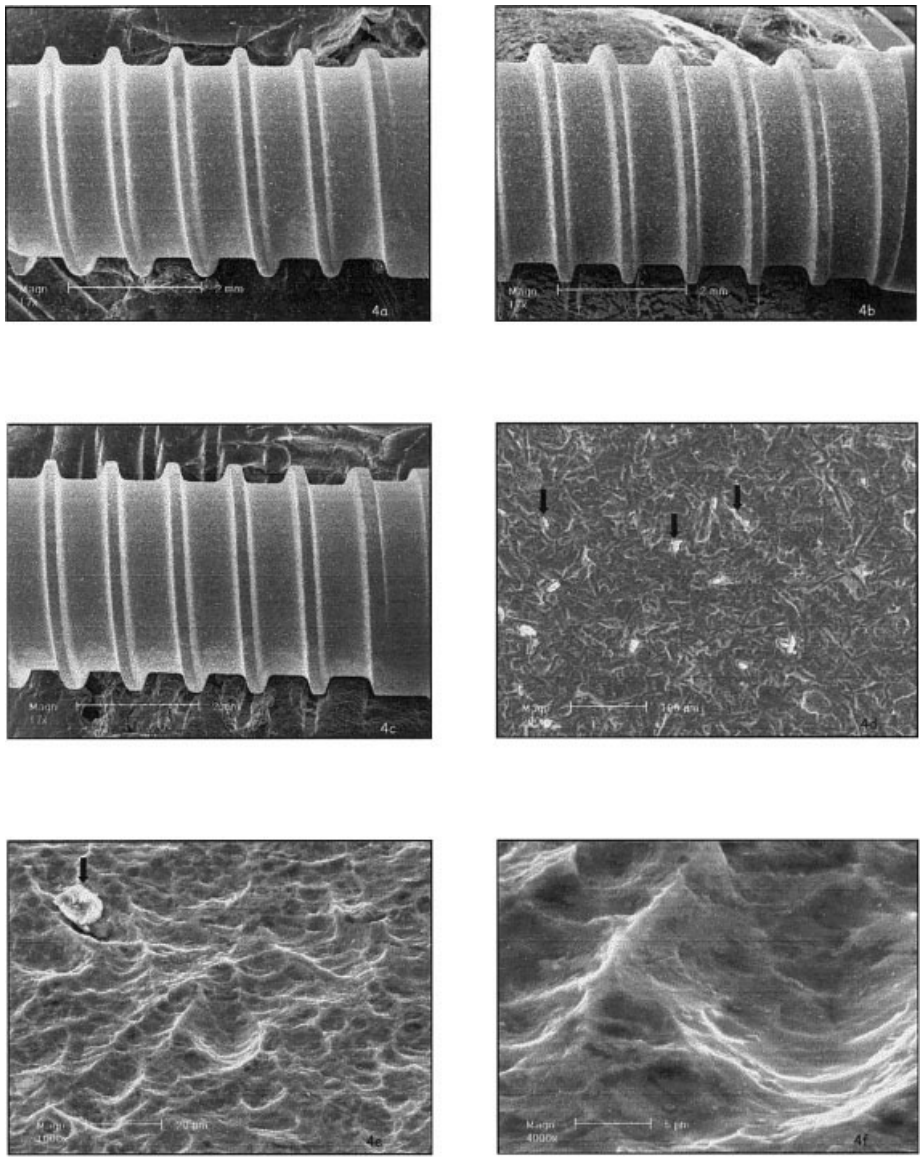

Figure 4. SEM micrographs of the HaTi implant surface. General overview of (a) the 11-mm-long implant, (b) the 14-mm-long implant, and (c) the 17-mm-long implant. The white spots correspond to alumina particles (× 17).(d) Surface topography showing remaining alumina (black arrows) particles (× 200). (e) Sandblasted and acid-attacked surface at higher magnification (× 1000). (f) At higher magnification (× 4000), the pits are wide and rounded, without undercuts.

in the advertising documents released by the manufacturer. This does not seem to interfere with the clinical performances of the implant[15,18] under standard healing conditions. The sand particles were more numerous and smaller than on the SLA surface; they were typically 2–10 μm and appeared weakly attached to the implant surface.

The features observed at the SLA implants were also unexpected. Mention of a MA transition zone between the implant neck and the SLA surface was not found either in the literature[3] or in the technical advertising documents released by the manufacturer. Therefore, this MA zone represents probably a shortage of the industrial process during the sandblasting step. The fact that the rough aspect and the amount of remaining sand varied for each implant issued from a different batch confirms that the industrial process can be improved. According to published clinical studies,[12,13,19] this lack of surface uniformity does not seem to interfere with the clinical performance.

The HaTi surface, although displaying a rough aspect at low magnification, showed wide and rounded pits at a higher magnification, instead of sharp ones. This pit shape is usually obtained by pickling (HF/HNO_3 acid attack) rather than by etching (HCl or HCl/H_2SO_4 acid attack), as described by Wilke et al.[5] These authors reported low torque values for various sandblasted-and-pickled surfaces inserted in bone for periods up to 1 year. Experimental studies should document if this surface has a bone interlocking capacity like other surfaces.[6,8]

The Osseotite surface is moderately etched, whereas the SLA surface presents deeper pits due to stronger etching conditions. The latter are able to create substantial pits even in the MA surface, sufficient for bone interlocking.[8] A difference in pit depth might explain the distinct torque patterns reported by Buser et al.[20] for SLA and Osseotite implants. Torquing the SLA implants resulted in a peak torque after 10–12 degrees that was followed by a steep reduction, whereas the torque applied at the Osseotite implants led to a flatter curve after 12-18° without a marked torque reduction.

All four implant surfaces have been acid attacked; nevertheless, due to the distinct treatment parameters, every implant displayed distinct surface roughness characteristics and a proper surface aspect that could not be mistaken. Seven distinct roughness parameters have been reported for each surface, including height, space, and hybrid descriptive data. However, their significance in terms of predicting an enhanced bone response or an increased implant fixation remains questionable. Wennerberg and Albrektsson[21] called for a detailed reporting on surface characterization, not limited to the classical height-descriptive (*Ra*, *Rq*, *Rz*, and *Rt*) parameters. However, the same authors stated that there is still uncertainty about which set of parameters, out of 13 listed roughness parameters, including height, space and hybrid descriptive data, is the most suitable for implant evaluation. Although the *Ra* is obviously insufficient by its own to characterize a given surface,[21,22] several studies reported a good correlation between increased *Ra* and stronger anchorage.[6,7,23] Wong et al.[6] evaluated pushed-out titanium cylinders placed in the knee trabecular bone of mini-pigs after 3 months. Four surfaces were compared; they were either blasted with glass, blasted with alumina, SLA treated, or plasma-sprayed with hydroxyapatite. The surface with the highest *Ra* showed the highest anchorage; a strong linear correlation, $r^2 = 0.90$, was found between the *Ra* and the push-out load. Similarly, Gotfredsen et al.[23] measured the anchorage of four treated surfaces in a rabbit tibia model after 4, 6, 9, and 12 weeks with the torque test. The surfaces were either machined, blasted with TiO_2 sand of various granulometry varying from 10–53 μm to 90–120 μm or titanium plasma sprayed (TPS). The highest torque values were observed at each time point for the roughest surface, as determined by the *Ra* and *Rt*. At all time points, these authors reported a high correlation of $r = 0.83$ between the *Ra* and implant anchorage. In that study, the skewness and kurtosis of the surfaces were also measured; however, these parameters did not correlate with implant anchorage. On the other hand, Chen et al.[24] studied the anchorage of simulated hips-stems topography in acrylic bone cement; they found the interfacial strength to increase monotonically with increase of the $R\Delta q$ instead of the *Ra*. Notably, a strong linear correlation, $r^2 = 0.98$, was found between the mean *Ra* and the mean $R\Delta q$ for the present four investigated implant surfaces. It is possible, however, that the recently described "apparent volume of interdigitation between implant surface and surrounding bone or cement"[25] is more suitable than other parameters to predict implant fixation.

It turns out that clinical implications cannot be drawn by relying on roughness-descriptive parameters alone. Nonetheless, biological and clinical data are available in the literature for the implants that displayed the lowest (Osseotite) and highest (SLA) height-descriptive parameters; they might provide some insight into the relationship between implant surface and biological and clinical behavior. Buser et al.[20] compared the torque resistance of Osseotite and SLA implants after 4, 8, and 12 weeks in the maxilla of mini-pigs. The SLA implants with a higher *Ra* (2.0 vs. 1.3 μm) were better anchored by 75–128%. Nevertheless, both surfaces displayed the same clinical advantages of textured surfaces; that is, short implants ($\leq$ 10 mm) do not have a higher propensity to fail than longer implants[8] and shorter healing periods of 6–8 weeks instead of 3–6 months are equally successful.[8] Szmukler-Moncler et al.[8] hypothesized that a threshold anchorage, which still remains to be determined, might be required to ensure the clinical advantages of textured surfaces, and that a marginal increase over this value might not have a clinical relevance. This threshold value would have been reached by surfaces that are capable of achieving the same predictability for short and longer implants, like the Osseotite,[14,26] TPS,[19] and SLA surfaces.[12,13,19]

The literature shows that when micromechanical anchorage is achieved, the bone-repair process switches from distance osteogenesis to contact osteogenesis,[27] and from slower bone corticalization around the implant surface to more rapid bone trabeculization and bone ingrowth into the rough surface.[1,28,29] In addition, because the bound mode is applicable in finite element analysis,[8] forces and strains at the interface are reduced and more evenly distributed along the implant surface.[30] This might explain why short implants can perform as well as longer implants.[14,19,31] In contrast, machined surfaces do not create micromechanical anchorage and bone interlocking;[23,31,32] bone response to machined surfaces is distance osteogenesis[27] and corticalization instead of trabeculization.[1,28,29] In finite-element analysis, the bound mode is not applicable;[8] forces and strains at the interface are of higher intensity, preferentially distributed at the tips of the threads and at the apex.[30] With this surface, short implants have been documented to fail more than longer ones,[31,33,34] and long healing periods have been recommended.[35] Therefore, it is possible that the clinical benefits of textured surfaces are not dictated, as previously suggested,[8,31] by a high level of anchorage per se. Rather the biological advantages of textured surfaces might be gained by the capacity of these surfaces to create a micromechanical anchorage with bone interlocking, which turns out to be a stronger implant fixation than for machined surfaces.[23,31]

Although higher *Ra* and stronger fixation have been correlated as mentioned above, a surface with a high *Ra* is insufficient by its own to warrant a high anchorage.[21,22] Bone interlocking requires the conjunction of a minimal *Ra* with peaks and/or valleys of adequate shape that permit bone ingrowth and bone retention. Despite its low *Ra*, the Osseotite surface showed a substantial bone anchorage at early healing stages,[7,20] and displayed the biological and

clinical advantages of textured surfaces,[14,26] probably because of the retentive capacity of the created pits. Subsequently, although the height-descriptive parameters of the DPS and the HaTi surfaces are significantly higher than the Osseotite surface, one cannot speculate on their biological performance until their bone interlocking capacity is demonstrated, especially for the surface with the rounded pits.

Based on the above, it is suggested that evaluation of bone-interlocking capacity should be used as a screening test for new textured surfaces that are developed to optimize the biological and clinical performances of implants.[8] Push-out or reverse-torque tests should demonstrate the presence of bone attached to the implant surface, such as the TPS,[23] SLA,[36] and MA[8] surfaces.

SUMMARY AND CONCLUDING REMARKS

In conclusion, treating titanium surfaces with acid does not create a standard topography. The latter varies according to several parameters, such as prior treatment, acid mixture composition, temperature, and time of acid treatment. In this survey, each implant system achieved a specific topography that could not be mistaken. This study revealed that (a) the industrial process is not fully reproducible and (b) manufacturer advertising on surfaces should be more accurate. Clinical implications based on roughness data alone cannot be extrapolated from one surface to another.

The authors are grateful to Professor Ivo Krejci (Dental School, University of Geneva, CH) for providing generous SEM access. SEM analysis has been professionally performed by Marie-Claude Reymond. Ing. Axel Baumann and Dr. Peter Zeggel (DOT GmbH, Rostock, D) are acknowledged for the roughness measurement on the implants.

REFERENCES

1. Buser D, Schenk RK, Steinemann SG, Fiorellini JP, Fox CH, Stich H. Influence of surface characteristics on bone integration of titanium implants: A histomorphometric study in miniature pigs. J Biomed Mater Res 1991;25:889–902.
2. Szmukler-Moncler S, Reingewirtz Y, Weber HP. Bone response to early loading: The effect of surface state. In: Davidovitch Z, Norton LA, editors. Biological mechanisms of tooth movement & craniofacial adaptation. Boston: Harvard Society for the Advancement of Orthodontics; 1996. p 611–616.
3. Cochran DL, Schenk RK, Lussi A, Higginbottom FL, Buser D. Bone response to unloaded and loaded titanium implants with a sandblasted and acid-etched surface: A histometric study in the canine mandible. J Biomed Mater Res 1998;40:1–11.
4. Szmukler-Moncler S, Perrin D, Ahossi V, Pointaire P. Evaluation of BONIT, a fully resorbable calcium phosphate (CaP) coating obtained by electrochemical deposition, after 6 weeks of healing: A pilot study in the pig maxilla. Key Eng Mater 2001;192–195:395–398.
5. Wilke HJ, Claes L, Steinemann S. The influence of various titanium surfaces on the interface shear strength between implants and bone. In: Heimke G, Soltész U, Lee AJC, editors. Clinical materials. Amsterdam: Elsevier; 1990. p 309–314.
6. Wong M, Eulenberger J, Schenk R, Hunziker E. Effect of surface topology on the osseointegration of implant materials in trabecular bone. J Biomed Mater Res 1995;29:1567–1575.
7. Klokkevold PR, Johnson P, Dadgostari S, Caputo A, Davies JE, Nishimura RD. Early endosseous integration enhanced by dual acid etching of titanium: A removal torque study in the rabbit. Clin Oral Implant Res 2001;12:350–357.
8. Szmukler-Moncler, S, Perrin D, Bernard JP, Pointaire P. Biological properties of acid etched titanium surfaces: Effect of sandblasting on bone anchorage. J Biomed Mater Res Appl Biomater (in press).
9. Lazzara RJ, Testori T, Trisi P, Porter SS, Weinstein RL. A human histologic analysis of Osseotite and machined surfaces using implants with 2 opposing surfaces. Int J Periodont Rest Dent 1999;19:3–16.
10. Baker DA, London RM, O'Neil RB. Rate of pull-out strength gain of dual-etched titanium implants: A comparative study in rabbits. Int J Oral Maxillofac Implants 1998:14:722–728.
11. Lazzara RJ, Porter SS, Testori T, Galante J, Zetterquist LA. A prospective multicenter study evaluating loading of Osseotite implants two months after placement. J Esthet Dent 1998;10: 280–289.
12. Roccuzzo M, Bunino M, Prioglio F, Bianchi SD. Early loading of sandblasted and acid etched (SLA) implants: A prospective split-mouth comparative study. Clin Oral Implant Res 2001;12: 572–578.
13. Cochran DL, Buser D, ten Bruggenkate C, Weingart D, Taylor TM, Bernard JP, Simpson JP, Peters F. The use of reduced healing times on ITI implants with a sandblasted and acid-etched (SLA) surface. Early results from clinical trials on SLA implants. Clin Oral Implant Res 2002;13:144–153.
14. Testori T, Del Fabbro, M, Feldman S, Vincenzi G, Sullivan G, Rossi R Jr, Anitua E, Bianchi F, Francetti L, Weinstein RL. A multi-center prospective evaluation of 2-months loaded Osseotite implants in the posterior jaws: 3-year follow-up results. Clin Oral Implant Res 2002;13:154–161.
15. Schulte W, d'Hoedt D, Axman D, Gomez-Roman G. 15 Jahre tübinger implantat und seine weiterentwicklung zum frialit-2-system. Z Zahnarzt Implantol 1992;8:77–96.
16. Beaty KD. U.S. Patent No..5,876,453. Implant surface preparation ; March 2, 1999.
17. Steinemann SG, Claes L. U.S. Patent No. 5,456,723. Metallic implant anchorable to bone tissue for replacing a broken or diseased bone; October 10, 1995.
18. Gomez-Roman G, Schulte W, d'Hoedt W, Axman-Kremar D. The Frialit-2 implant system: Five-year clinical experience in single tooth and immediately post-extraction applications. Int J Oral Maxillofac Implants 1997;12:299–309.
19. Nedir R, Bischof M, Briaux JM, Beyer S, Szmukler-Moncler S, Bernard JP. A 7-year life table analysis from a prospective study on ITI implants with special emphasis on the use of short implants. Results from a private practice. Clin Oral Implant Res (in press).
20. Buser D, Nydegger T, Hirt HP, Cochran DL, Nolte LP. Removal torque values of titanium implants in the maxilla of miniature pigs. Int J Oral Maxillofac Implants 1998;13:611–619.
21. Wennerberg A, Albrektsson T. Suggested guidelines for the topographic evaluation of implant surfaces. Int J Oral Maxillofac Implants 2000;15:331–344.
22. Hansson S. Surface roughness parameters as predictors of anchorage strength in bone : a critical analysis. J Biomech 2000; 23:1297–1303.
23. Gotfredsen K, Berglundh T, Lindhe J. Anchorage of titanium implants with different surface characteristics: An experimental study in rabbits. Clin Implant Dent Relat Res 2000;2:120–128.
24. Chen CQL, Scott W, Barker TM. Effect of metal surface topography on mechanical bonding at simulated total hip stem-

cement interfaces. J Biomed Mater Res Appl Biomater 1999; 48:440–446.
25. Arola DD, Yang DT, Stoffel KA. The apparent volume of interdigitation: A new parameter for evaluating the influence of surface topography on mechanical interlock. J Biomed Mater Res Appl Biomater 2001;58:519–524.
26. Testori T, Wiseman L, Woolfe S, Porter SS. A prospective multicenter clinical study of the Osseotite implant: Four-year interim report. Int J Oral Maxillofac Implants 2001;16:193–200.
27. Davies JE. Mechanisms of endosseous integration. Int J Prosthodont 1998;11:391–401.
28. Gross U, Muller-Mai CM, Fritz T, Voigt C, Knarse W, Schmitz HJ. Implant surface roughness and mode of load transmission influence peri-implant bone structure. In: Heimke G, Soltész U, Lee AJC, editors. Clinical materials. Amsterdam: Elsevier; 1990. p 303–308.
29. Muller-Mai CM, Voigt C, Gross U, Berger G. Bone development and bone structure depend on surface roughness and structure of metallic implants. In: Wise D, editor. Biomaterials and bioengineering handbook. New York: Marcel Dekker; 2000. p 457–481.
30. Van Oosterwyck H, Duyck J, Vander Sloten J, Van der Perre G, De Cooman M, Lievens S, Puers R, Naert I. The influence of bone mechanical properties and implant fixation upon bone loading around oral implants. Clin Oral Implant Res 1998;9: 407–418.
31. Bernard JP, Szmukler-Moncler S, Pessotto S, Vazquez L, Belser UC. The anchorage of Brånemark and ITI implants of various lengths. I. An experimental study in the canine mandible. Clin Oral Implant Res 2003;14:593–600.
32. Sennerby L, Thomsen P, Ericson LE. Ultrastructure of the bone–titanium interface in rabbits. J Mater Sci Mater Med 1992;3:262–271.
33. Lazzara R, Siddiqui AA, Binon P, Feldman SA, Weiner R, Philipps R. Gonshor A. Retrospective multicenter analysis of 3i endosseous dental implants placed over a 5-year period. Clin Oral Implant Res 1996;7:73–83.
34. Esposito M, Hirsch JM, Lekholm U, Thomsen P. Biological factors contributing to failures of osseointegrated oral implants. (I). Success criteria and epidemiology. Eur J Oral Sci 1998;106: 527–551.
35. Senneby L, Roos J. Surgical determinants of clinical success of osseointegrated implants: A review of literature. Int J Prosth 1998;11:408–420.
36. Buser D, Nydegger T, Oxland TR, Schenk RK, Cochran DL, Snétivy D, Nolte LP. The interface shear strength of titanium implants with a sandblasted and acid-etched surface. A biomechanical study in the maxilla of miniature pigs. J Biomed Mater Res 1999;45:75–83.